Balance Control of a Humanoid Robot using the Inclinometer

Kui-Hong Park, Jun Jo and *Jong-Hwan Kim
School of Information Technology, Gold Coast campus, Griffith University,
PMG 50, Gold Coast Mail Centre, Australia
{k.park, junjo}@griffith.edu.au, *johkim@rit.kaist.ac.kr
*Department of EECS, Korea Advanced Institute of Science and Technology (KAIST),
Guseong-dong, Yuseong-gu, Daejeon, 305-701, Republic of Korea

Abstract

In this paper, the inclinometer is used to control the balance of a humanoid robot on a miniature surfboard. GHR (**G**riffith University **H**umanoid **R**obot) is the humanoid robot developed in the Robotics and Games laboratory, at Griffith University. In order to measure the angle of the inclining surfboard, the inclinometer is attached to the back of the right foot of the GHR. To remove the high frequency data, LPF (Low Pass Filter) is adopted. Using the angle information of the inclinometer, GHR makes the proper motion on the moving surfboard.

Keywords: balance control, humanoid robot, inclinometer, moving average filter

1 Introduction

A humanoid robot is a biped intelligent robot. It is anticipated that this type of robot will eventually become a real human companion in the future. Recently, researchers have been focusing on developing humanoid robots which are similar in many aspects to human beings [1,2,3,4,5,6].
Since a biped robot inherently suffers from problems like instability and balance, and is at constant risk of falling down, ensuring stability should be considered the most important goal from the perspective of locomotion. To measure stability, the concept based on ZMP (Zero Moment Point) proposed by Vukobratovic [7] is used. The ZMP is defined to be the point on the ground plane at which the total moments due to ground contacts becomes zero. It is important to recognize that ZMP must always reside in the convex hull of all contact points on the ground plane, since the moments on the ground plane are caused only by normal forces at the contact points which are always positive in the upper vertical direction. In addition to ZMP, the angle or movement of the humanoid robot is measured to stabilize the motion. For this purpose, the inclinometer, accelerator and gyro were used [8, 9]. Sometimes, the kalman filter and complementary filter were adopted to get the exact angle information of the humanoid robot [10, 11].

In this paper, a balance control scheme based on the geometry calculation is applied to a biped robot. To remove the noise information, several filters are used and compared.

Section 2 presents the humanoid robot, GHR (Griffith Humanoid Robot). In section 3, the control algorithm for balance control of the GHR is presented. The experimental results and comparisons between median filter and moving average filter are described. Concluding remarks follow in Section 5.

2 GHR

2.1 Hardware specification

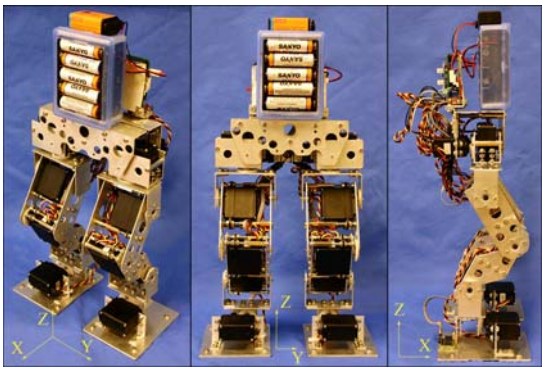

Figure 1: GHR

GHR was developed by the Robotics and Games laboratory at Griffith University as a test bed. GHR was equipped with 12 RC servo motors for its actuator and 2-axis inclinometer. Figure 1 shows the angle-front, front and side views of the GHR.

Figure 2: SCA100T

Table 1: Hardware specification

Height	29cm (lower body only)
Weight	about 1.5kg
Actuator	12 RC servo motors - 6 motors per leg (HS-5945MG)
Controller	ATmega128
Sensor	SCA100T (2-axis inclinometer)
Power	8.4V Ni-MH for logic, 1.2V/2300mAh x 5 per each leg

In order to detect the inclining angle of GHR, SCA100T was attached to the back of of the right foot. SCA100T can measure the dual axis inclination at the same time ($\pm$ 90^o ($\pm$ 1g)). Figure 2 shows the SCA100T module [12].

The microcontroller, ATmega128, controls the 12 RC servo motors every 20ms. The sensor information from the SCA100T is measured by using the internal A/D converter of the microcontroller every 20ms.

2.2 Simulator

The robot motion was developed and refined by using a specific motion simulator developed at Griffith University. Currently, this is an off-line control where each actuator follows the pre-defined data. Figure 3 shows the simulator for the humanoid robot.

Figure 3: Simulator for GHR

Various movements or motions of GHR, such as walking, turning, side-walking and kicking, can be generated using this simulator. The output of the simulator is the motion file and is used in other control programs for the GHR.

3 Control Algorithm

For the balance control, the miniature surfboard was prepared as shown in figure 4.

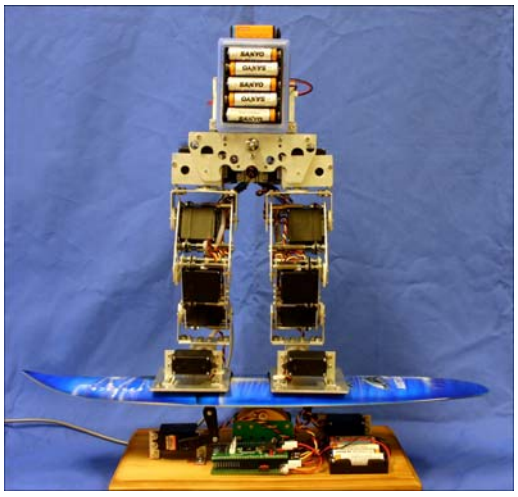

Figure 4: Experimental environment

To balance on the moving surfboard, the one leg needs to be extended, or stretched out and the other leg, bent. The geometry method is employed for calculating the variation of the length. Figure 5 shows the initial pose of GHR before the balance control. As shown in Figure 5, L_1 is the length between hip and knee and L_2 is the length between knee and ankle, respectively. HY, KY and AY represent the angle of actuators in the hip y, the knee y and the ankle y, respectively. HY_0, KY_0, AY_0, α_0 and β_0 are the constant values. Before the surfboard starts to swing, GHR stands on the flat surfboard as shown in Figure 4. The arrows around the hip, knee and ankle joints in Figure 5 depict the moving direction of each actuator. Both legs have the same moving direction in the absolute coordinates as shown in Figure 1.

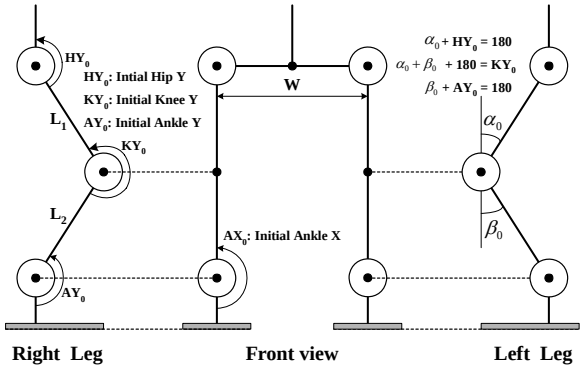

Figure 5: Initial pose of GHR on the surfboard

When the surfboard starts to incline, GHR implements the appropriate motion to maintain its balance on the surfboard as shown in Figure 6.

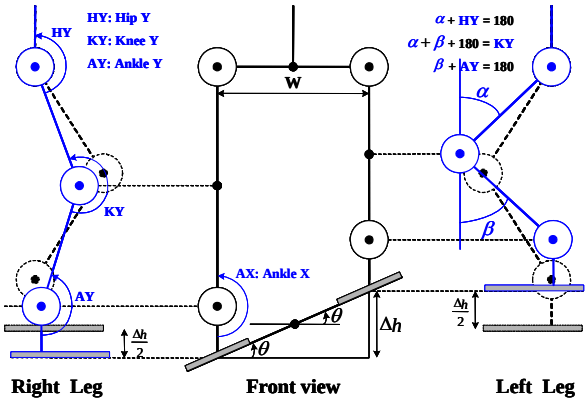

Figure 6: Proper pose of GHR on the surfboard

To achieve the appropriate pose of GHR on the inclining surfboard, the geometry calculation is employed. When the surfboard is inclined at the angle θ, the variation of the height between the two legs is Δh. Considering only the left leg, the desired angle α and β are calculated, respectively, as follows:

$$\begin{aligned}\frac{\Delta h}{2} &= \frac{W}{2}\tan\theta \\ &= (L_1\cos\alpha_0 + L_2\cos\beta_0) - (L_1\cos\alpha + L_2\cos\beta) \\ &= L_1(\cos\alpha_0 - \cos\alpha) + L_2(\cos\beta_0 - \cos\beta)\end{aligned} \quad \textbf{(1)}$$

In equation (1), there are two terms. One is the variation term from the length L_1 and angle α and the other is the variation term from the length L_2 and angle β. Assuming that the magnitude of the both variations are the same, the desired angles α and β can be calculated as below:

$$\begin{aligned}&\frac{W}{4}\tan\theta = L_1(\cos\alpha_0 - \cos\alpha) = L_2(\cos\beta_0 - \cos\beta) \\ &\therefore \alpha = \cos^{-1}(\cos\alpha_0 - \frac{W}{4L_1}\tan\theta), \\ &\beta = \cos^{-1}(\cos\beta_0 - \frac{W}{4L_2}\tan\theta)\end{aligned} \quad \textbf{(2)}$$

In Figure 5 and 6, the control inputs of GHR are the Hip Y, the Knee Y and the Ankle Y. The variations of these control inputs are calculated by using the relationship between the control inputs and the desired angles α and β.

$$\begin{aligned}&\mathrm{HY} = 180 - \alpha, \\ &\mathrm{KY} = 180 + \alpha + \beta, \\ &\mathrm{AY} = 180 - \beta\end{aligned} \quad \textbf{(3)}$$

These control inputs are used for the left leg. The RC servo motors of the y-axis in right leg have the opposite alignment of that of the left leg. For the y-axis actuator in the right leg, the variations of the control inputs of the y-axis in the left leg are calculated.

$$\begin{aligned}&\mathrm{RHY} = \mathrm{RHY}_0 - \Delta HY \\ &\mathrm{RKY} = \mathrm{RKY}_0 - \Delta KY \\ &\mathrm{RAY} = \mathrm{RAY}_0 - \Delta AY\end{aligned} \quad \textbf{(4)}$$

In equation (4), RHY, RKY and RAY are the right hip y, the right knee y and the right ankle y, respectively. RHY_0, RKY_0 and RAY_0 are the initial right hip y, the initial knee y and the initial ankle y, respectively. For the ankle x in both legs, the measured inclining angle of the surfboard is used directly.

$$\mathrm{LAX} = \mathrm{RAX} = \theta \quad \textbf{(5)}$$

In equation (5) LAX and RAX are the left ankle x and the right ankle x, respectively.

4 Experimental Result

Two RC servo motors are used to create an artificial wave which can simulate the movement of the surfboard on the ocean. The RC servo motors are connected to the surfboard as shown in Figure 4. These motors can generate a triangular wave. To reduce the high frequency data, two kinds of filters are adopted. One is the median filter and the other is the moving average filter [13]. Both filters are frequently implemented in image processing to remove the noise.

$$y[i] = \mathrm{median}(x_{i-N+1}, x_{i-N+2}, \mathrm{K}\ , x_{i-1,} x_i) \quad \textbf{(6)}$$

$$y[i] = \frac{1}{N}\sum_{j=0}^{N-1} x[i-j] \quad \textbf{(7)}$$

Equations (6) and (7) express the median filter and the moving average filter, respectively. In both equations, x_i is the input data and y_i is the filtered output data. In equation (6), *median* means the median value of several samples. In real implementations, N is set to 10.

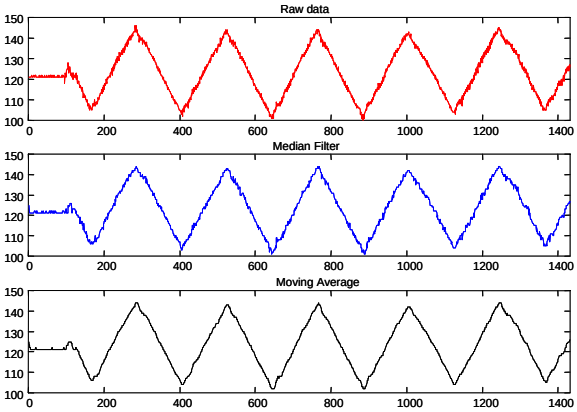

Figure 7: The measured data before the balance data

Figure 7 shows the measured data and filtered data before the balance control. X-axis value is the number of data and y-axis value is the magnitude of the measured and filtered data. As shown in Figure 7, the

measured data (raw data) from the SCA100T reflects the movement of the surfboard. In Figure 7, the raw data and filtered data appear the same. However, on inspection of the narrow section of the data, a difference between the raw data and the filtered data can be seen. Figure 8 shows the 300 samples of the data taken from what is shown in the Figure 7. In the raw data, high frequency data exists. On close inspection, of the data of both the filtered outputs, the data from the moving average filter can be seen to be superior to the median filter data.

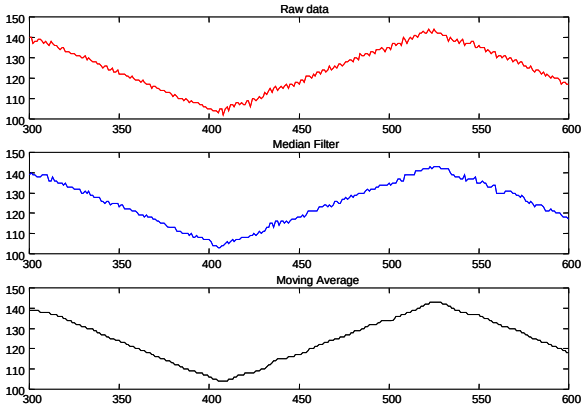

Figure 8: 300 data sample before the balance control

In equation (2), α_0 and β_0 are the constant values. Thus, the value of $\cos^{-1}\alpha_0$ and $\cos^{-1}\beta_0$ are also constant values. These constant values make the offset values inside of the $\cos^{-1}$ function. Due to the effect of these offset values, the variation range of α and β are restricted. For this reason, in the real experiment, equation (2) is modified to become equation (8). This equation form is obtained through the real experiment.

$$\therefore \alpha = \cos^{-1}(-\frac{W}{4L_1}\tan\theta) + (\alpha_0 - 90), \qquad (8)$$
$$\beta = \cos^{-1}(-\frac{W}{4L_2}\tan\theta) + (\beta_0 - 90)$$

Using equation (3), (4), (5) and (8), the balance control can be implemented for the humanoid robot.

Also, the sensor data measured during the balance control is shown in Figure 9, which also shows the measured and filtered data.

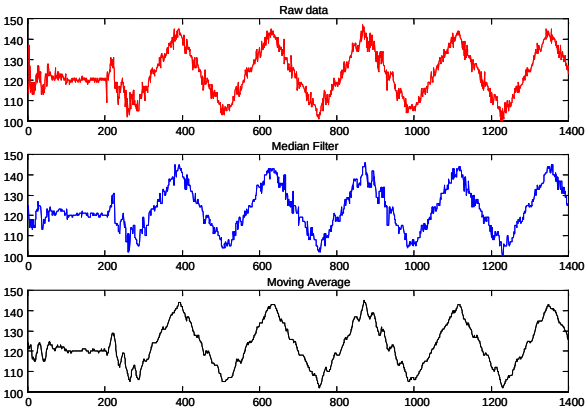

Figure 9: The data measured during balance control

The ankle of GHR is controlled by using the sensor information. This means that the foot is controlled by using the equations (4) and (5). Thus, the measured data from the sensor located on the foot has more high frequency data than without the balance control. Therefore, by comparison with Figure 7, more high frequency data exists during the balance control. Figure 10 shows the 300 samples of the data taken from what is shown in figure 9.

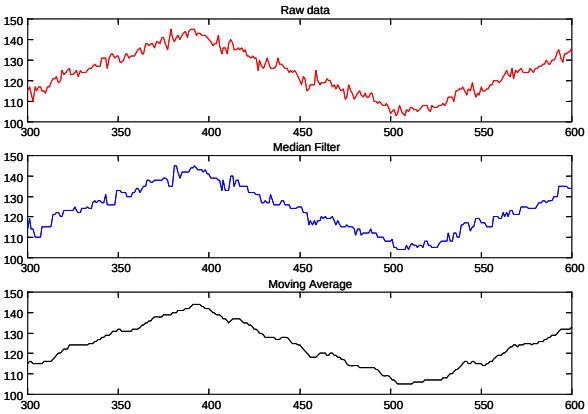

Figure 10: 300 data sample during the balance control

As the Figure 7, the output data from the moving average filter has less high frequency data. Figure 11 shows the desired angles α and β by using equation (8). In this case, the inclining angle θ was the output data from the moving average filter. The x-axis value is the number of the data and the y-axis value is the magnitude of the angle.

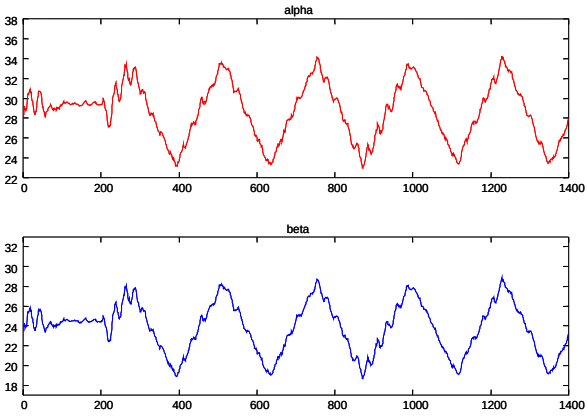

Figure 11: Calculated desired angles α and β

For the data collected and represented in Figure 12, the artificial wave was generated by hand and the sensor data was measured. Figure 12 shows the measured data and filtered data and Figure 13 shows the 500 samples of the data in the figure 12, respectively.

As shown in Figures 8, 10 and 13, the moving average filter reduces the high frequency data. Figure 14 shows the desired angles α and β when the artificial wave is generated by the hand.

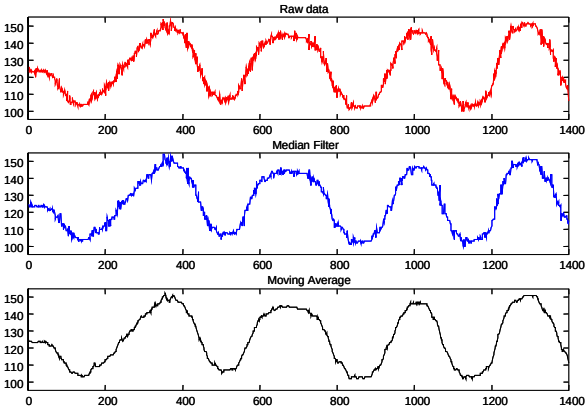

Figure 12: The measured data using the hand

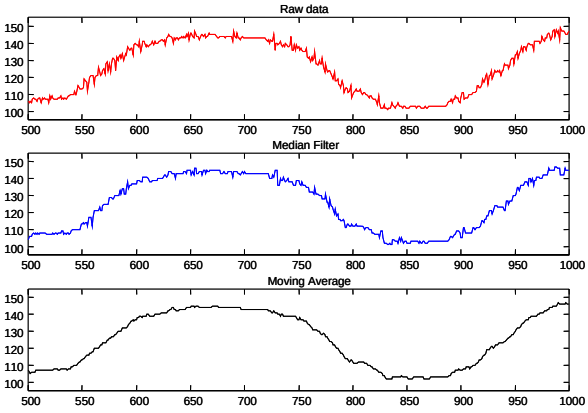

Figure 13: 500 data sample using the hand

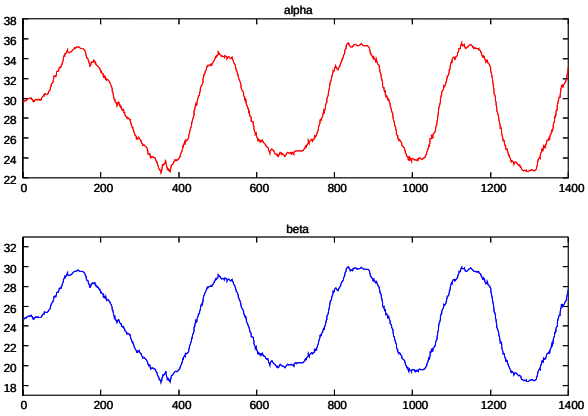

Figure 14: Calculated desired angles α and β

Figure 15 shows the experimental result without the balance control. In this case, GHR almost fell off the miniature surfboard.

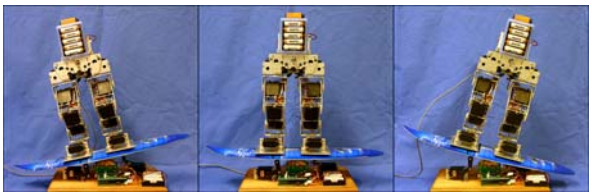

Figure 15: Without the balance control

Figure 16 shows the robot's motion with balance control.

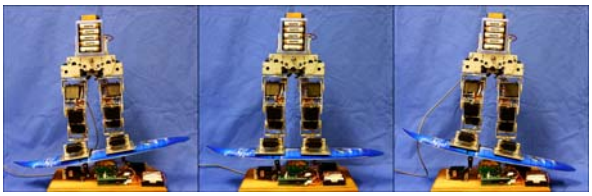

Figure 16: With the balance control

As shown in Figure 16, GHR made the appropriate movements to maintain balance on the inclining surfboard. Figure 17 shows the stretching and bending of the leg of GHR during the balance control.

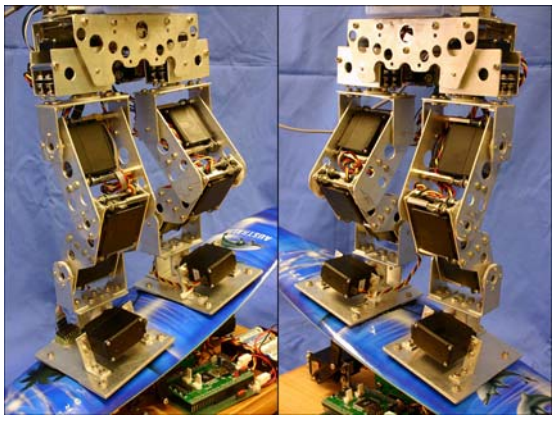

Figure 17: Leg stretching and folding

5 Conclusion

GHR is the humanoid robot developed by the Robotics and Games laboratory at Griffith University and used as a test bed. To measure the inclining angle, GHR was equipped with a 2-axis inclinometer. The median filter and the moving average filter were adopted to reduce the high frequency data from the measured data. Comparing the filtered output data, the performance of the moving average filter was verified in this application. In this paper, the inclinometer, SCA100T, was implemented and used to provide GHR, a humanoid robot, with the ability to maintain balance on a moving miniature surfboard. The experimental results were reported showing how the balance control for GHR was achieved using the inclinometer.

6 Acknowledgement

SCA100T was supported by VTI technologies without payment. This work was supported by the ITRC-IRRC (Intelligent Robot Research Center) of the Korean Ministry of Information and Communication in 2005.

7 References

[1] K. Hirai, M. Hirose, Y. Haikawa, and T. Takenaka, "The Development of Honda Humanoid Robot," Proc. of IEEE Int. Conf. on Robotics and Automations, pp. 1321-1326, 1998.

[2] J. Yamaguchi, A. Takanishi, and I. Kato, "Development of a biped walking robot compensating for three-axis moment by trunk motion," Proc. of IEEE/RSJ Int. Conf. on Intelligent Robots and Systems, pp. 561-566, 1993.

[3] Y. Sakagami, R. Watanabe, C. Aoyama, S. Matsunaga, N. Higake, and K. Fujimura, "The intelligent ASIMO: System overview and integration," Proc. of IEEE/RSJ Int. Conf. On Intelligent Robots and Systems, pp. 2478-2483, 2002.

[4] K. Nishiwaki, T. Sugihara, S. Kagami, F. Sanehiro, M. Inaba, and H. Inoue, "Design and Development of Research Platform for Perception-Action Integration in Humanoid Robot: H6," Proc. of IEEE/RSJ Int. Conf. on Intelligent Robots and Systems, pp. 1559-1564, 2000.

[5] J.-H. Kim, D.-H. Kim, Y.-J. Kim, K.-H. Park, J.-H. Park, C.-K. Moon, K. T. Seow, and K.-C. Koh, "Humanoid Robot HanSaRam: Recent Progress and Development," Journal of Advanced Computational Intelligence & Intelligent Informatics, vol. 8, no. 1, pp. 45-55, 2004.

[6] J.-H. Kim, J.-H. Oh, "Walking Control of the Hummanoid Platform KHR-1 based on Torque Feedback Control," Proc. of IEEE International Conference on Robotics and Automation, pp. 623-628, 2004.

[7] M. Vukobratovic and D. Juricic, "Contribution to the Synthesis of Biped Gait," IEEE Trans. on Bio-Medical Engineering, vol. BME-16, no. 1, pp. 1-6, 1969.

[8] Ishida, T., "Development of a Small biped Entertainment Robot QRIO," Proc. of the 2004 International Symposium on Micro-Nanomechatronics and Human Science, and The Fourth Symposium Micro-Nanomechatronics for Information-Based Society, pp. 23-28, 2004.

[9] K. Loffler, M. Gienger, F. Pfeiffer, and H. Ulbrich, "Sensors and control concept of a biped robot," Industrial Electronics, IEEE Transactions on vol. 51, Issue 5, pp. 972-980, 2004.

[10] M. Gienger, K. Loffler and F. Pfeiffer, "Practical Aspects of Biped Locomotion," Experimental Robotics VIII, STAR 5, pp. 95-104, 2003.

[11] T. Nagasaki; S. Kajita, K. Kaneko, K. Yokoi and K. Tanie, "A Running Experiment of Humanoid Biped," Proc. of IEEE/RSJ Int. Conf. On Intelligent Robots and Systems, pp. 136-141, 2004.

[12] VTI Technology, "Home Page", http://www.vti.fi visited on 15/1/2005.

[13] A.V. Oppenheim and R.W. Schafer, "Digital Signal Processing," Prentice Hall.